

# Robust Adaptive Cerebellar Model Articulation Controller for 1-DOF Nonlaminated Active Magnetic Bearings

Ngoc Hoi LE, Thanh Quyen NGO, Dinh Khoi HOANG, Quang Dich NGUYEN, Duc Thinh LE, Tung Lam NGUYEN\*

**Abstract:** This paper presents a robust adaptive cerebellar model articulation controller (RACMAC) for 1-DOF nonlaminated active magnetic bearings (AMBs) to achieve desired positions for the rotor using a robust sliding mode control based. The dynamic model of 1-DOF nonlaminated AMB is introduced in fractional order equations. However, it is challenging to design a controller based on the model's parameters due to undefined components and external disturbances such as eddy current losses in the actuator, external disturbance, variant parameters of the model while operating. In order to tackle the problem, RACMAC, which has a cerebellar model to estimate nonlinear disturbances, is investigated to resolve this problem. Based on this estimation, a robust adaptive controller that approximates the ideal and compensation controllers is calculated. The online parameters of the neural network are adjusted using Lyapunov's stability theory to ensure the stability of system. Simulation results are presented to demonstrate the effectiveness of the proposed controller. The simulation results indicate that the CMAC multiple nonlinear multiple estimators are close to the actual nonlinear disturbance value, and the effectiveness of the proposed RACMAC method compared with the FOPID and SMC controllers has been studied previously.

**Keywords:** cerebellar model; electromagnetic bearing; nonlinear external disturbances; robust adaptive control

## 1 INTRODUCTION

AMB is an electromechanical device that employs magnetic field to levitate and manipulate the rotor position to prevent physical contact between the rotor and stator. The system, therefore, has no friction or abrasion. Besides the fact that it does not need to be lubricated, electromagnetic bearing also has a long lifespan and hence can reduce environmental pollution. It has been used widely in many applications and areas such as transportation, aerospace, energy, and high-technology, i.e. high-speed CNC machines [1-3]. Exhibiting its precious advantage in high-speed applications, it is preferable to use non-laminated AMB over laminated one due to its physical strength and endurance.

One of the significant problems when controlling the nonlaminated AMB is that the dynamic model of the system is affected by nonlinear disturbances, i.e., eddy current losses in the actuator, external disturbance, and variant parameters of the model while operating. Hence it is difficult to establish an accurate mathematical model for the system, which decreases the effectiveness of model-based control approaches. In contrast, using their learning capability, intelligent control methods can generally eliminate the effect of variant parameters or unknown disturbances. Moreover, they also remove the necessity of knowing detailed information about the system during the design process.

Along with the development of the AMB system, in the past decades, there have been many classic control methods such as PID control, modern control such as optimal control, adaptive control, sustainable control and nonlinear controls such as Backstepping control, and sliding mode control. Especially in recent years, intelligence such as fuzzy control, adaptive PID control, and neural network control [4-10] has been developed and applied to control the desired position of the rotor in a conventional magnetic bearing (AMB) system where the actuator has a layered structure. For the case of non-laminated magnetic drive [11-14] almost no research on intelligent control in general and neural network on control in particular has been published. The authors only apply

classical control methods to frequency domains such as PID, FOPID [15], FBL [16], FBL-PID [16]. Especially for a non-laminated magnetic bearing actuator containing a fractional derivative that represents eddy current losses in the actuator, while the magnetic bearing is composed of thin engineered steel sheets. Often ignore eddy currents and dynamics that do not contain fractional quantities. On the other hand, the problem of control for objects whose dynamics contain exponential derivatives is a relatively new problem, developed only within the last decade.

Due to the response to the PID, FOPID, and SMC controllers [17] can be considered to satisfy the requirements of the drive from the non-laminated structure when considering the system to work without changing model parameters over time. However, magnetic bearing is an object with uncertain parameters, and this is a limitation that PID, FOPID, and SMC controllers cannot overcome. Therefore, to overcome the disadvantages of RACMAC, the traditional PID, FOPID and SMC controllers are replaced to stabilize the non-laminated magnetic drive system. Since then, the comparison results between the proposed RACMAC and the conventional control methods PID, FOPID and SMC have been studied for the drive from the original structure. The results show that the proposed method for the quality is suitable for the drive better disturbance variation than PID, FOPID, FBL and SMC.

The new contributions of the paper can be summarized as follows:

(i) In this study, we have successfully built a mathematical model on the time domain of the non-laminated active magnetic bearing structure under the total nonlinear disturbance, including external load force acting on the rotor, model uncertainty, and disturbances due to eddy current loss.

(ii) RACMAC structure including CMAC to estimate the nonlinear disturbance and ideal controller approximation based on the robust sliding mode control is proposed for AMBs. Thanks to advantages such as flexible adjustment of network parameters, fast response and good adaptation to changing nonlinear disturbances, RACMAC overcomes the disadvantages of traditional controllers such as PID and FOPID.

(iii) The simulation results demonstrate the advantages of the proposed RACMAC and show the superior response of the proposed controller in terms of adapting to changes in nonlinear disturbance better than FOPID [22], and SMC [17] studied for non-laminated magnetic drives.

The paper is organized as follows: Section II briefly describes the mathematical model of 1-DOF nonlaminated AMB. Section III.1 presents the scheme of RACMAC used in this work to control the rotor position of the nonlaminated AMB. The detailed designing procedure will be outlined in Section III.2. The adaptive learning rules of RACMAC are constructed based on Lyapunov's stability theory [23], [24] to ensure the convergence of the network and the observability of the system in the closed-loop control system. Then in Section IV, the simulation results of the nonlaminated AMB system in the case of having external disturbances will be given to demonstrate the capability of the proposed RACMAC. Finally, our conclusion and discussion are provided in Section V.

## 2 MATHEMATICAL MODEL

Consider a nonlaminated electromagnetic C-shaped stator as shown in Fig. 1 [15-19].

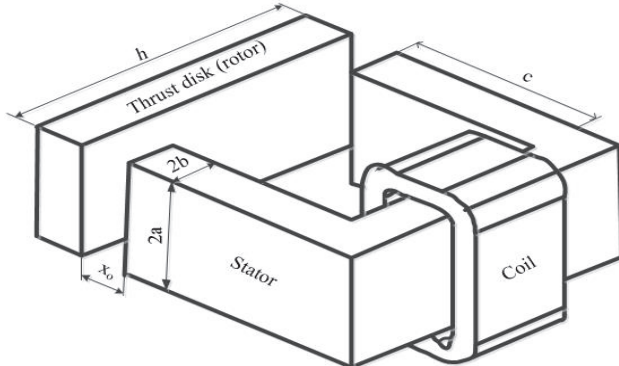


Figure 1 Nonlaminated AMB C-shaped

The structure of the control system is illustrated in Fig. 1. It consists of a rotor attached freely at the desired distance  $x_0$  to the electromagnetic actuator (stator), and a distance sensor measures the deviation  $x$  between the actual position of the rotor and the desired position  $x_0$ . The controller then uses this information to calculate a control signal to keep the rotor at the desired position, which means to balance the gravitational force  $F_g = mg$  of the rotor and all external forces  $F_L$  applied in the vertical plane. The control signal is then transferred to the amplifier to generate an alternative current for the electromagnetic actuator. This current creates an electromagnetic force  $F_{dt}$  to maintain the position of the rotor. In general, the control law actions as follows: when the rotor moves downward from the desired position, a signal is generated from the controller to increase the electromagnetic force to pull the rotor upward and vice versa. According to [11-14], [18] the nonlaminated electromagnetic force in the frequency domain is described as follows:

$$F(s) = K_i \frac{R^0}{R^0 + k\sqrt{s}} I(s) + K_x \frac{R^0}{R^0 + k\sqrt{s}} X(s) \quad (1)$$

where  $s = j\omega$  denotes the Laplace operator,  $I(s)$  and  $X(s)$  are the control current and the deviation between the desired position and the actual position in the frequency domain. The eddy current coefficient is expressed:

$$k = \left[ \frac{l_i}{4(a+b)} + \frac{b}{3a} - \frac{64b^2}{\pi^5 a^2} \tan h\left(\frac{\pi a}{2b}\right) \right] \sqrt{\frac{\sigma}{\mu_r \mu_0}} \quad (2a)$$

where  $a$  is half-height of magnetic pole,  $b$  is half-width of magnetic pole. The length of magnetic field line  $l_i$  is  $l_i = 2h + 2c$ ,  $\mu_r$  is relative permittivity,  $\mu_0$  vacuum permittivity,  $\sigma$  is the conductivity of iron,  $c$  is length of stator,  $h$  is Length of rotor (Fig. 1). The static coil's resistance  $R^0$  is:

$$R^0 = \frac{1}{\mu_0 A} \left( 2x_0 + \frac{l_i}{\mu_r} \right) \quad (2b)$$

where  $A = 4ab$  is the area of cross section of the magnetic pole,  $x_0$  is the length of the gap between stator and rotor. The proportional current coefficient  $K_i$  is:

$$K_i = \frac{2N^2 i_0}{\mu_0 A (R^0)^2} \quad (2c)$$

The coefficient proportional to the deviation  $K_x$

$$K_x = \frac{1}{(R^0)^3} \left( \frac{2Ni_0}{\mu_0 A} \right)^2 \quad (2d)$$

where  $N$  is the number of wires,  $i_0$  denotes bias current. Then, the electromagnetic force in the frequency domain Eq. (1) is rewritten as follows:

$$F(s) + \frac{k\sqrt{s}}{R^0} F(s) = K_i I(s) + K_x X(s) \quad (3)$$

Taking the inverse Laplace transform of Eq. (3), the electromagnetic force in time domain  $F(t)$  is obtained as follows:

$$F(t) + \frac{k}{R^0} \frac{d^{1/2} F(t)}{dt^{1/2}} = K_i i + K_x x \quad (4)$$

where  $i$  is the control current in time domain.  $x$  is the deviation between the desired position and the real position in time domain. Based on the second Newton's law, the dynamic equation of the C-shaped can be described as:

$$m \frac{d^2 x}{dt^2} = F(t) - mg + F_L \quad (5)$$

where  $F_L$  is the external disturbances Load,  $m$  is the rotor's mass, and  $g$  denotes the gravitational acceleration. From Eq. (5) and Eq. (4), we have

$$\begin{aligned} \frac{d^2x}{dt^2} &= \frac{1}{m} \left( \frac{k}{R^0} \frac{d^{1/2}F(t)}{dt^{1/2}} - K_i i - K_x x \right) - g + \frac{F_L}{m} = \\ &= f(x, t) + g(i_0) i + d(x, t) \end{aligned} \quad (6)$$

where

$$\begin{aligned} f(x, t) &= -\frac{1}{m} (K_x x + mg), \quad g(i_0) = \frac{K_i}{m}, \\ d(x, t) &= \frac{1}{m} \left( \frac{k}{R^0} \frac{d^{1/2}F(t)}{dt^{1/2}} + F_L \right) \end{aligned}$$

Notice that  $d(x, t)$  is a nonlinear dynamic function that is difficult to determine precisely. Therefore, it is difficult to design a model-based controller to respond well. In addition, the actual value  $f(x, t), g(i_0)$  can be divided to the nominal component  $f_0(x, t), g_0(i_0)$  and the parameter uncertainties  $\Delta f_0(x), \Delta g_0(i_0)$ . Then, the Eq. (6) becomes:

$$\begin{aligned} \frac{d^2x}{dt^2} &= [f_0(x, t) + \Delta f_0(x, t)] + [g_0(i_0) + \Delta g_0(i_0)] i + \\ &\quad + d(x, t) = f_0(x, t) + g_0(i_0) i + l(x, t) \end{aligned} \quad (7)$$

#### Assumption 1.

$l(x, t)$  is the nonlinear disturbance component that is limited by a positive constant  $L_{cc}$  as follows:

$$l(x, t) \leq L_{cc} \quad (8)$$

### 3 RACMAC DESIGN

#### 3.1 Structure of Ideal Controller

The controller's objective is to keep the rotor position  $x$  close to the input signal  $x_d$ . Thus, defining the error is as follows:

$$e = x_d - x \quad (9)$$

The sliding surface of the error integral is defined as

$$s = \dot{e} + k_1 e + k_2 \int_0^t e(\tau) d\tau \quad (10)$$

The ideal controller is designed as follows:

$$i_{id} = \frac{1}{g_0(i_0)} \left[ \ddot{x}_d - f_0(x, t) - l(x, t) + K^T E \right] \quad (11)$$

where  $K = [k_1 \ k_2]^T$ ,  $E = [\dot{e} \ e]^T$

From Eqs. (9) to (11), the time derivative of the sliding surface is obtained as follows:

$$\dot{s} = 0 \quad (12)$$

It can be seen from Eq. (12) that the error will equal zero. However, the ideal controller in Eq. (11) cannot be determined since we do not precisely know  $l(x, t)$ . To resolve this problem, we propose a control scheme that comprises a CMAC and a compensation controller designed as follows:

$$i = i_{CMAC} + i_{CC} \quad (13)$$

where  $i_{CMAC}$  is used to approximate the ideal controller  $i_{id}$  and  $i_{CC}$  is designed to achieve robust tracking performance.

#### 3.2 Ideal Controller Approximation Using CMAC

The main purpose of CMAC is to estimate the nonlinear disturbance  $l(x, t)$ , which includes: the fractional derivative of the nonlaminated electromagnetic force, external disturbances, and uncertain parameters. From Eq. (6) and Eq. (7), the disturbances can be rewritten as follows:

$$l(x, t) = \Delta f_0(x, t) + \Delta g_0(i_0) i + d(x, t) \quad (14)$$

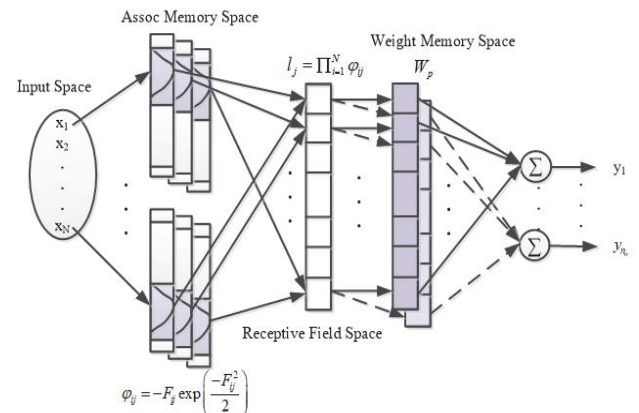


Figure 2 Structure of CMAC

As shown in Fig. 2, CMAC consists of five spaces: input space, association memory space, receptive field space, weight memory space, and output space. The main function of each space is summarized as below:

1) Input space: The input of CMAC. The input vector is defined as  $x = [x_1, x_2, \dots, x_N]$ , where  $N$  is the number of input signals.

2) Association memory space: each block in the association memory space contains an activation function of CMAC and it has several layers. In this work, we use the wavelet function

$$\varphi_{ij} = -F_{ij} \exp\left(\frac{-F_{ij}^2}{2}\right) \quad (15)$$

$$F_{ij} = \frac{x_i - o_{ij}}{v_{ij}} \quad (16)$$

where  $o_{ij}$  and  $v_{ij}$  are the center and width of the activation function of the  $i$ -th input and  $j$ -th layer,  $j = 1, 2, \dots, n$ .

3) Receptive field space: with input  $x$ , the receptive function can be described as

$$l_j = \prod_{i=1}^N \varphi_{ij} \quad (17)$$

4) Weight memory space: This space determines the adjusted gain of the output of weight memory space:

$$W_p = \begin{bmatrix} W_{1p}, & W_{2p}, & \dots, & W_{np} \end{bmatrix}^T, p = 1, 2, \dots, n_0 \quad (18)$$

5) Output space: the output of CMAC is:

$$y_p = W_p^T l \quad (19)$$

where

$$W_p = \begin{bmatrix} w_{11} & \dots & w_{1n_l} \\ \dots & \ddots & \dots \\ w_{p1} & \dots & w_{pn_l} \end{bmatrix}; l = \begin{bmatrix} l_1 \\ \vdots \\ l_{n_l} \end{bmatrix}$$

Define the optimized control law for the ideal controller as follows:

$$i_{id} = W^{*T} L^* + \Delta \quad (20)$$

where  $\Delta$  is approximated error and  $W^*$ ,  $L^*$  are the matrices and vectors of the optimized parameters of  $W$ ,  $L$ , respectively. In general, verifying these matrices and vectors for the ideal controller is unrealistic. Hence, we use  $i_{CMAC}$  as the online estimated value of  $i_{id}$ . The estimated function of the control law for  $i_{CMAC}$  is defined as:

$$i_{CMAC} = \hat{W}^T \hat{L} \quad (21)$$

where  $\hat{W}$ ,  $\hat{L}$  are the estimated matrix and vector of  $W^*$ ,  $L^*$ . The estimated error is then calculated as:

$$\begin{aligned} \tilde{i} &= i_{id} - i_{CMAC} \\ &= W^{*T} L^* + \Delta - \hat{W}^T \hat{L} \\ &= \tilde{W}^T \tilde{L} + \hat{W}^T \hat{L} + \tilde{W}^T \hat{L} + \Delta \end{aligned} \quad (22)$$

where  $\tilde{W} = W^* - \hat{W}$  and  $\tilde{L} = L^* - \hat{L}$ . Here Taylor expansion is used to approximate a nonlinear function to a linear one:

$$\tilde{L} = L_o \tilde{o} + L_v \tilde{v} + \zeta \quad (23)$$

where:

$$\begin{aligned} L_o &= \left[ \frac{\partial L_1}{\partial o} \quad \frac{\partial L_2}{\partial o} \quad \dots \quad \frac{\partial L_{n_l}}{\partial o} \right]_{o=o} \\ L_v &= \left[ \frac{\partial L_1}{\partial v} \quad \frac{\partial L_2}{\partial v} \quad \dots \quad \frac{\partial L_{n_l}}{\partial v} \right]_{v=v} \end{aligned}$$

$\zeta$  is the high-order component. Substituting Eq. (23) into Eq. (22) we obtain:

$$\begin{aligned} \tilde{i} &= \tilde{W}^T \tilde{L} + \hat{W}^T (L_o \tilde{o} + L_v \tilde{v} + \zeta) + \tilde{W}^T \hat{L} + \Delta \\ &= \tilde{W}^T \tilde{L} + \hat{W}^T L_o \tilde{o} + \hat{W}^T L_v \tilde{v} + \hat{W}^T \zeta + \tilde{W}^T \hat{L} + \Delta \\ &= \hat{W}^T L_o \tilde{o} + \hat{W}^T L_v \tilde{v} + \tilde{W}^T \hat{L} + \varepsilon \end{aligned} \quad (24)$$

where:  $\varepsilon = \hat{W}^T \zeta + \tilde{W}^T \tilde{L} + \Delta$  is an uncertain parameter.

### Assumption 2.

The uncertain parameter  $\varepsilon$  is assumed that bound in positive constant  $K_{cc}$ .

$$0 \leq \varepsilon \leq K_{cc} \quad (25)$$

The robust tracking controller is defined as follows:

$$i_{CC} = K_{cc} \operatorname{sgn}(s) \quad (26)$$

For the SMC controller, the sigmoid switch function is used to reduce the chattering:

$$\operatorname{Sigmoid}(s) = \frac{2}{1 + e^{-sa}} - 1 \quad (27)$$

### 3.3 Stability Analysis

**Theorem 1.** Consider the nonlaminated active magnetic bearings described in detail in Eqs. (1) to (7) and bounded unknown disturbance mentioned in Assumption 1 and Assumption 2. Then, the system obtains stability according to the Lyapunov theorem and Barbalat's lemma by using the control law Eq. (21), and the robust tracking controller Eq. (26).

**Proof:** To demonstrate the stability of the control system, we define a Lyapunov candidate function as

$$V = \frac{1}{2} s^2 + \frac{1}{2v_w} \operatorname{tr}(\tilde{W}^T \tilde{W}) + \frac{1}{2v_o} \tilde{o}^T \tilde{o} + \frac{1}{2v_v} \tilde{v}^T \tilde{v} \quad (28)$$

Differentiating Eq. (28) and using Eq. (24), Eq. (26) lead to

$$\begin{aligned} \dot{V} &= ss - \frac{1}{v_w} \operatorname{tr} \left( \tilde{W}^T \dot{\tilde{W}} \right) - \frac{1}{v_o} \tilde{o}^T \dot{\tilde{o}} - \frac{1}{v_v} \tilde{v}^T \dot{\tilde{v}} \\ &= \sum_{j=1}^{n_l} \tilde{W}_{jp}^T (s \hat{L} - \frac{1}{v_w} \hat{W}_{jp}) + \tilde{o}^T \left( s L_o^T \hat{W} - \frac{1}{v_o} \dot{\tilde{o}} \right) \\ &\quad + \tilde{v}^T \left( s L_v^T \hat{W} - \frac{1}{v_v} \dot{\tilde{v}} \right) + s\varepsilon - si_{CC} \end{aligned} \quad (29)$$

Eq. (29) suggest that the adaptive law is calculated as follows:

$$\dot{\hat{W}}_{jp} = v_w s \hat{L} \quad (30)$$

$$\dot{o} = v_o s L_o^T \hat{W} \quad (31)$$

$$\dot{v} = v_v s L_v^T \hat{W} \quad (32)$$

where  $v_o$ ,  $v_v$ , and  $v_w$  are small positive constants used to adjust the learning speed. Substituting Eqs. (30) to (32) into (29) yields:

$$\begin{aligned} \dot{V} &= s\varepsilon - sK_{CC}\text{sgn}(s) \\ &= s(\varepsilon - K_{CC}\text{sgn}(s)) \end{aligned} \quad (33)$$

From the Eq. (25) and Eq. (26), the Eq. (33) obtains  $\dot{V} \leq 0$ . According to the Lyapunov theorem and Barbalat's lemma, we can conclude that the closed-loop system with the proposed RACMAC is globally asymptotically stable.

## 4 SIMULATION EVALUATION

### 4.1 Simulation Setting

In this section, we present the simulation results of the proposed RACMAC scheme on a nonlaminated electromagnetic with the dynamic model, as shown in Fig. 3. The system's parameters are chosen as in Tab. 1.

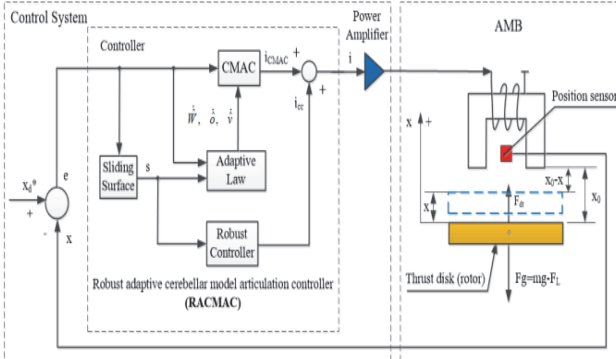


Figure 3 Structure of the control system proposed RACMAC for nonlaminated AMB C-shaped

Table 1 Parameters of the nonlaminated electromagnetic bearing

Parameters	Symbol	Value
Half-height of magnetic pole	$a$	7.5 mm
Half-width of magnetic pole	$b$	2.5 mm
Length of stator	$c$	20 mm
Length of rotor	$h$	30 mm
Conductivity of iron	$\sigma$	$2.5 \times 10^6$ S/m
Relative permittivity	$\mu_r$	5000
Vacuum permittivity	$\mu_0$	$4\pi \times 10^{-7}$ T.m/A
Mass of rotor	$m$	2.25 kg
Length of the gap between stator and rotor	$x_0$	0.2 mm
Number of wires	$N$	1200
Bias current	$i_0$	0.2 A
Area of cross section of magnetic pole	$A$	$75 \times 10^{-6}$ m <sup>2</sup>
Maximum current in the magnetic pole	$i_{max}$	1A
Static magnetic resistance	$R^0$	$4.4563 \times 10^6$ A/Wb
Current coefficient	$K_i$	307.7479 N/A
Displacement coefficient	$K_x$	$2.9309 \times 10^5$ N/m
Eddy coefficient	$k$	$5.1619 \times 10^4$ A/Wb

To evaluate the advantages of RACMAC, we compared the proposed controller with the conventional

sliding mode control and the fractional-order PID (FOPID) presented in [15, 19, 20]. We use the FOMCON toolbox of MATLAB [19] to simulate the FOPID controller. The RACMAC uses the parameters shown in Tab. 2.

Table 2 Parameters of RACMAC

Parameters	Symbol	Value
Center of activation function	$o$	[-0.1 ... 0.1]
Width of activation function	$v$	0.2
Number of layers	$n_l$	25
Weight of memory	$w$	80
Bound of estimated error	$K_{ce}$	0.0001
Gain coefficient K	$k_1, k_2$	2500, 12500
Learning speed	$v_o, v_v, v_w$	1

In order to demonstrate the effectiveness of the controller, the simulation is performed with two scenarios as follows:

**Scenario 1:** Force the rotor from the initial position ( $x_0 = -0.2$  mm) acto track to the sinusoidal signal with a frequency of 6 Hz. At time  $t = 0.2$  s, there is an external load disturbance  $F_L = 6$  N acting on the rotor, model uncertainty, and the fractional derivative of the nonlaminated electromagnetic force.

**Scenario 2:** Drive the rotor from the initial position ( $x_0 = -0.2$  mm) to track the desired signal  $x_d = 0$ . At time  $t = 0.2$  s, there is a sinusoidal increase in external load disturbance:  $F_L = 150\sin(100t)$  acting on the rotor, the uncertainty and the fractional derivative of the nonlaminated electromagnetic force are added.

## 4.2 Simulation Result and Discussion

### 4.2.1 Result of Scenario 1

Simulation results for the proposed RACMAC in comparison with classical FOPID controller ( $PI^{\lambda}D^{\mu}$ ) for the case are shown in Figs. 4 to 7. According to Fig. 4, the total nonlinear disturbance is relatively small. The CMAC estimate closely follows the actual total nonlinear disturbance value. Only after 0.02 s since the initial transient, the nonlinear disturbance, which is just disturbance caused by eddy currents in the actuator, is quite small and since 0.2 s, when there are many externals and model parameters change the value. The estimated value is also very close to the actual nonlinear disturbance value. Since 0.2 s, when there is the external disturbance and the model's parameter uncertainty affects the rotor, the total disturbance has increased by about 6 (N/kg).

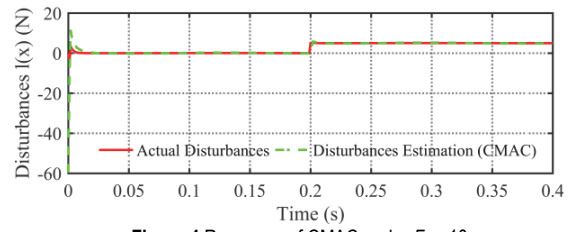
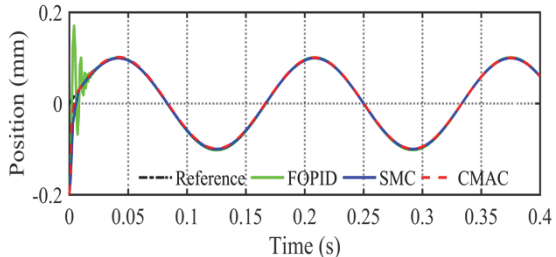
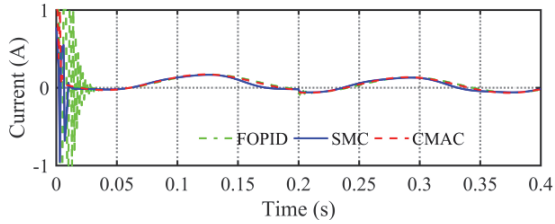
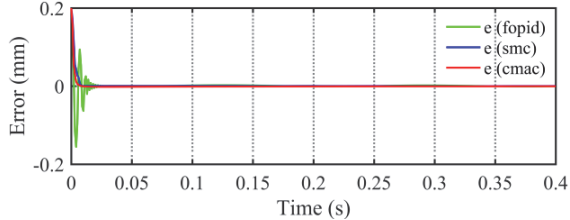


Figure 4 Response of CMAC under  $F_L = 10$

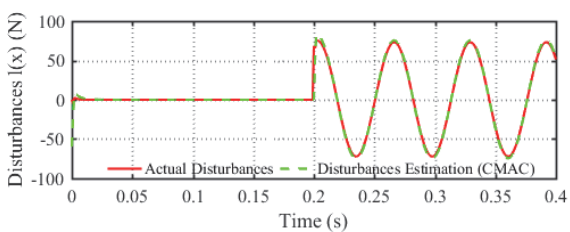
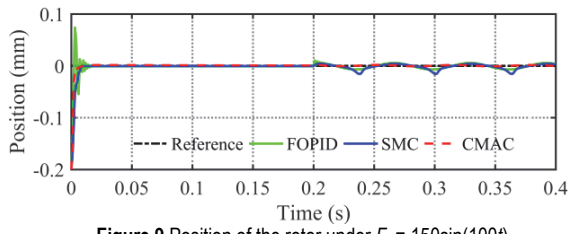
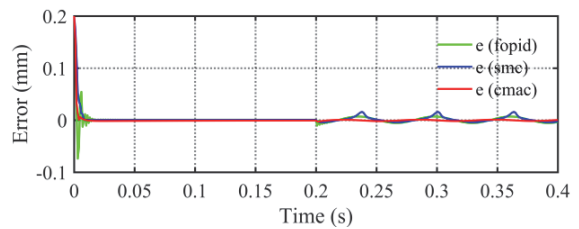
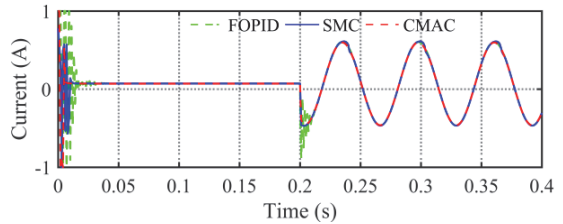
The position and error are shown in Figs. 5, 7 and Tab. 2 for the case where the set signal is sinusoidal. As can be observed, the rotor using the proposed controller responds fast and only takes 0.005 s to reach the designed position. At the time  $t = 0.2$  s when the load disturbance of the model

is added, due to the small magnitude of the load disturbance, both RACMAC, SMC and FOPIID still stick to the set position, and the oscillation of the signal is small.

Figure 5 Position of the rotor under  $F_L = 10$ Figure 6 Control current of the system under  $F_L = 10$ Figure 7 Error of the rotor under  $F_L = 10$ 

#### 4.2.2 Result of Scenario 2

The results are shown in Figs. 4 to 11, in the same Scenario 1, the simulation results of the position response and the error of the rotor position under two control actions are shown in Figs. 8 to 11. According to Fig. 8, the results are similar to case 1. The estimated disturbance value of CMAC closely follows the actual nonlinear disturbance value in a short time for both periods without nonlinear disturbance (0-0.2 s), and the period with external disturbance acting on (0.2-0.4 s later), but the disturbance value is more significant than Scenario 1.

Figure 8 Response of CMAC under  $F_L = 150\sin(100t)$ Figure 9 Position of the rotor under  $F_L = 150\sin(100t)$ Figure 10 Error of the rotor under  $F_L = 150\sin(100t)$ Figure 11 Control current of the system under  $F_L = 150\sin(100t)$ 

#### 4.2.3 Discussion

The results of the parameters showing the quality of RACMAC compared to FOPIID and SMC are shown in Tabs. 3 and 4. From the results shown in Tabs. 2 and 3, the authors found that the parameters of quality of the kit The proposed RACMAC controller is better than traditional controllers such as FOPIID and SMC, specifically as follows: For PID, the overshoot is quite large, for RACMAC, it is not available. The values such as distance deviation, settling time, and maximum error of RACMAC have a smaller value than FOPIID and SMC, thus it can be confirmed that the proposed controller has better control quality than traditional controllers such as FOPIID and SMC, especially in terms of the disturbances. From this, RACMAC has improved performance and can adapt to the disturbances better than other controllers like FOPIID and SMC. This also shows the advantages of RACMAC and proves that our proposed controller is promising in controlling the nonlaminated AMB system.

Table 3 Output values of controllers under Scenario 1

Value	FOPIID	SMC	CMAC
Overshoot	149 $\mu\text{m}$	No	No
Distance tracking error average	7.45 $\mu\text{m}$	1.95 $\mu\text{m}$	1.90 $\mu\text{m}$
Settling time	0.03 s	0.01 s	0.005 s
Maximum tracking error	230 $\mu\text{m}$	24.30 $\mu\text{m}$	1.73 $\mu\text{m}$

Table 4 Output values of controllers under Scenario 2

Value	FOPIID	SMC	CMAC
Overshoot	155 $\mu\text{m}$	no	no
Distance tracking error average	8.50 $\mu\text{m}$	3.50 $\mu\text{m}$	2.28 $\mu\text{m}$
Settling time	0.03 s	0.01 s	0.005 s
Maximum tracking error	320.53 $\mu\text{m}$	32.28 $\mu\text{m}$	2.60 $\mu\text{m}$

## 5 CONCLUSION

This paper presents a RACMAC scheme to control the rotor position of the 1-DOF nonlaminated AMB and apply it successfully to the simulated system to acquire the desired position of the rotor. The significant advantage of the proposed control scheme is that the dynamic model does not need to be fully acknowledged and requires no

strict restrictions. CMAC estimates nonlinear disturbances such as eddy current loss, friction, external disturbance, and variant parameters of the model. We also present the stability proof of the controller using Lyapunov's theory. The simulated results show that the electromagnetic bearing can respond to changing the input trajectory under the condition of disturbances. Simulation results compared with SMC and FOPIID show that the RACMAC method proposed performs better than SMC and FOPIID under external disturbance and parameter uncertainties. In the future, the 1-DOF nonlaminated AMB model will be further analysed using Ansys Maxwell software and experimental results are also targeted.

## Acknowledgments

This research is funded by Industrial University of Ho Chi Minh City (IUH) under research project code 22/1D01. The authors would like to thank Industrial University of Ho Chi Minh City (IUH) for this support.

## 6 REFERENCES

- [1] Inman, J. & Brown, V. (1998). Adaptive Bearing Variable Control Bias Magnetic. <https://doi.org/10.1109/ACC.1998.703021>
- [2] Cho, H. W., Kim, C. H., Lee, J. M., & Han, H. S. (2011). Design and characteristic analysis of small scale magnetic levitation and propulsion system for maglev train application. *2011 International Conference on Electrical Machines and Systems, ICEMS 2011*. <https://doi.org/10.1109/ICEMS.2011.6073910>
- [3] Kaloust, J., Ham, C., Siehling, J., Jongekryg, E., & Han, Q. (2004). Nonlinear robust control design for levitation and propulsion of a maglev system. *IEE Proceedings - Control Theory and Applications*, 151(4), 460-464. <https://doi.org/10.1049/ipta:20040547>
- [4] Fei, J. & Hou, S. (2012). Robust adaptive fuzzy control for three-phase active power filter. *2012 IEEE 13th Workshop on Control and Modeling for Power Electronics, COMPEL 2012*, 61074056. <https://doi.org/10.1109/COMPEL.2012.6251725>
- [5] Chen, H. C. (2008). Optimal fuzzy pid controller design of an active magnetic bearing system based on adaptive genetic algorithms. *Proceedings of the 7th International Conference on Machine Learning and Cybernetics, ICMLC*, 4(July), 2054-2060. <https://doi.org/10.1109/ICMLC.2008.4620744>
- [6] Matsumura, F. & Yoshimoto, T. (1986). System Modeling and Control Design of a Horizontal-Shaft Magnetic-Bearing System. *IEEE Transactions on Magnetics*, 22(3), 196-203. <https://doi.org/10.1109/TMAG.1986.1064296>
- [7] Chen, S. Y. & Lin, F. J. (2011). Robust nonsingular terminal sliding-mode control for nonlinear magnetic bearing system. *IEEE Transactions on Control Systems Technology*, 19(3), 636-643. <https://doi.org/10.1109/TCST.2010.2050484>
- [8] Dimond, T., Allaire, P., Mushi, S., Lin, Z., & Yoon, S. Y. (2012). Modal tilt/translate control and stability of a rigid rotor with gyroscopes on active magnetic bearings. *International Journal of Rotating Machinery*, 2012. <https://doi.org/10.1155/2012/567670>
- [9] Chen, S. C. & Tung, P. C. (2000). Application of a rule self-regulating fuzzy controller for robotic deburring on unknown contours. *Fuzzy Sets and Systems*, 110(3), 341-350. [https://doi.org/10.1016/S0165-0114\(98\)00190-0](https://doi.org/10.1016/S0165-0114(98)00190-0)
- [10] Chen, S. C., Nguyen, V. S., Le, D. K., & Nam, N. T. H. (2014). Nonlinear control of an active magnetic bearing system achieved using a fuzzy control with radial basis function neural network. *Journal of Applied Mathematics*, 2014. <https://doi.org/10.1155/2014/272391>
- [11] Zhu, L., Knospe, C. R., & Maslen, E. H. (2005). Analytic model for a nonlaminated cylindrical magnetic actuator including eddy currents. *IEEE Transactions on Magnetics*, 41(4), 1248-1258. <https://doi.org/10.1109/TMAG.2005.844847>
- [12] Zhu, L. & Knospe, C. R. (2010). Modeling of nonlaminated electromagnetic suspension systems. *IEEE/ASME Transactions on Mechatronics*, 15(1), 59-69. <https://doi.org/10.1109/TMECH.2009.2016656>
- [13] Knospe, C. R. & Zhu, L. (2011). Performance limitations of non-laminated magnetic suspension systems. *IEEE Transactions on Control Systems Technology*, 19(2), 327-336. <https://doi.org/10.1109/TCST.2010.2044179>
- [14] Zhu, L., Knospe, C., & Maslen, E. (2006). A Complete Model for Solid Cylindrical Magnetic Actuators. *10th International Symposium on Magnetic Bearings*. <https://doi.org/10.1109/TMAG.2005.844847>
- [15] Ou, B., Song, L., & Chang, C. (2010). Tuning of fractional PID controllers by using radial basis function neural networks. *2010 8th IEEE International Conference on Control and Automation, ICCA 2010*, 1239-1244. <https://doi.org/10.1109/ICCA.2010.5524367>
- [16] Whitlow, Z. W. (2014). Modeling and Control of Non-laminated Active Magnetic Thrust Bearings. *Scholar Archive Org.*, (December), 1-72. <https://doi.org/10.18130/V3NT0G>
- [17] Gosiewski, M. & Źokowski, Z. (2006). Sliding Mode Control for Active Magnetic Bearings. *18th International Symposium on Magnetic Bearings*, (August). <https://doi.org/10.13140/RG.2.2.22406.88646>
- [18] Seifert, R., Röbenack, K., & Hofmann, H. (2019). Rational Approximation of the Analytical Model of Nonlaminated Cylindrical Magnetic Actuators for Flux Estimation and Control. *IEEE Transactions on Magnetics*, 55(12). <https://doi.org/10.1109/TMAG.2019.2936791>
- [19] Tepljakov, A., Petlenkov, E., & Belikov, J. (2011). FOMCON: a MATLAB Toolbox for Fractional-order System Identification and Control. *International Journal of Microelectronics and Computer Science*, 2(2), 51-62.
- [20] Yeroglu, C., Onat, C., & Tan, N. (2009). A new tuning method for  $P\lambda D\mu$  controller. *ELECO 2009 - 6th International Conference on Electrical and Electronics Engineering*, 312-316. <https://doi.org/10.1109/ELECO.2009.5355344>
- [21] Couzon, P. Y. & Der Hagopian, J. (2007). Neuro-fuzzy active control of rotor suspended on active magnetic bearing. *Journal of Vibration and Control*, 13(4), 365-384. <https://doi.org/10.1177/1077546307074578>
- [22] Chen, S. C., Nguyen, V. S., Le, D. K., & Nam, N. T. H. (2014). An online trained adaptive neural network controller for an active magnetic bearing system. *Proceedings - 2014 International Symposium on Computer, Consumer and Control, IS3C 2014*, 741-744. <https://doi.org/10.1109/IS3C.2014.197>
- [23] Schilling, R. J. (1998). *Fundamentals of Robotics: Analysis and control*. Hoboken, NJ: Prentice-Hall.
- [24] Slotine, J. J. E. & Li, W. (1991). *Applied Nonlinear Control*. Hoboken, NJ: Prentice-Hall.

## Contact information:

### Ngoc Hoi LE

- 1) Industrial University of Ho Chi Minh City, Vietnam
- 2) Hanoi University of Science & Technology, Vietnam

### Thanh Quyen NGO

- Industrial University of Ho Chi Minh City, Vietnam

**Dinh Khoi HOANG**

Industrial University of Ho Chi Minh City, Vietnam

**Quang Dich NGUYEN**

Hanoi University of Science & Technology, Vietnam

**Duc Thinh LE**

Hanoi University of Science & Technology, Vietnam

**Tung Lam NGUYEN**

(Corresponding author)

Hanoi University of Science & Technology, Vietnam

E-mail: lam.nguyentung@hust.edu.vn

#### Acronyms

RACMAC	Robust Adaptive Cerebellar Model Articulation Controller
SMC	Sliding Mode Control
AMB	Active Magnetic Bearings
PID	Proportional Integral Derivative
FOPID	Fractional Order Proportional Integral Derivative
FBL	Feedback Linearization